Physical Basics and Industrial Applications of 3MA – Micromagnetic Multiparameter Microstructure and Stress Analysis[1]

Gerd DOBMANN

Fraunhofer IZFP, Germany

Abstract. Micromagnetic NDT techniques like the measurement of the magnetic Barkhausen noise, the incremental permeability and the harmonic analysis of the tangential magnetic field allow deriving inspection procedures to online monitoring and control machinery parts and components in production processes in order to characterize mechanical properties like hardness, hardening depth, yield and tensile strength. These types of inspection procedures continuously were further developed in the last two decades so that today the forth generation of system hard and software is in industrial use. The application is in steel industry where steel sheets in hot-dip-galvanizing lines were annealed after cold rolling but also in heavy plate rolling mills where after thermo-mechanical rolling special textures and texture gradients can occur. An increasing number of applications are also to find in the machinery building industry and here especially in case of machinery parts of the car supplying industry. The contribution introduces in the methodology of the micromagnetic, multiparameter, microstructure and stress analysis (3MA), which, however, only can be applied at ferromagnetic materials and describes the physical basics of the techniques. The applied technology is especially sensitive for mechanical property determination as the relevant microstructure is governing the material behavior under mechanical loads (strength and toughness) in a similar way as the magnetic behavior under magnetic loads, i.e. during the magnetization in a hysteresis loop. In different case studies the advantage to implement 3MA into the industrial processes is discussed.

Keywords. Micromagnetic NDE, hardness, hardening depth, residual stresses, yield strength, steel industry, steel sheets, heavy plates, machinery building, automotive.

[1] A shorter version of the paper was presented at the ENDE2007 conference, held in Cardiff, UK, June 19-21, 2007 and has been accepted for publication by the IOS Press publishing house.

Introduction

The reason to develop 3MA (Micromagnetic-, Multiparameter-, Microstructure-, and stress-Analysis), starting in the late seventies in the German nuclear safety program, was to find microstructure sensitive NDT techniques to characterize the quality of heat treatments, for instance the stress relieve of a weld. George Matzkanin [1] just has had published a NTIC report in the USA to the magnetic Barkhausen noise. The technique was sensitive to microstructure changes as well as to load-induced and residual stresses. Therefore a second direction of research started in programs of the European steel industry and the objective was to determine residual stresses in big steel forgings, like turbine shafts. Beside the magnetic Barkhausen effect also a magneto-acoustic-one became popular [2]. The technique has based on acoustic emission measurements during a hysteresis cycle and was – because of the high amplification – also sensitive to electric interference noise. Therefore the acoustic Barkhausen noise technique has never found a real industrial application. Later further micromagnetic techniques were developed: the incremental permeability measurement, the harmonic analysis of the magnetic tangential field and the measurement of the so-called dynamic or incremental magnetostriction by use of an EMAT [3, 4].

1. Physical Basics

Ferromagnetic materials - even in a demagnetized or so called virgin state - consist of small, finite regions called domains [5-8]. Each domain is spontaneously magnetized to the saturation value M_s of the material. The directions of magnetization of the various domains, however, are such that the specimen as a whole shows no net magnetization. The process of magnetization is then one of converting the multi-domain state into a single domain magnetized in the same direction as the applied magnetic field H. The process is performed not continuously but stepwise by movement of the domain walls, the so called Bloch walls, and for stronger applied fields, by rotation of the magnetization vectors in the domains into the direction of the applied field. In iron-based materials we find 180° and 90° Bloch walls. The indicated angle is the angle between the magnetization vectors in two adjacent domains. Domains with directions parallel or nearly parallel to the magnetizing field increase in their size while all others are annihilated. The Bloch wall movements also called Bloch wall jumps take place discontinuously because the walls are temporarily pinned by microstructural obstacles like dislocations, precipitates, phase- or grain-boundaries in a polycrystalline material. The stepwise pull-out of the wall from the obstacle changes the magnetization state locally and is called a Barkhausen event. The local magnetization changes induce pulsed eddy currents in the vicinity of the events with frequency spectra in the range dc $\leq f \leq$ 2 - 3 MHz propagating in all spatial directions. The amplitudes of the eddy currents are damped according to a well known dispersion law $\propto \sqrt{f}$, i.e. higher frequencies in the spectrum are damped more than lower frequencies. The eddy currents induce electrical voltage pulses, i.e. the so called Barkhausen noise which may be detected by an induction coil surrounding the magnetized specimen. The time domain integral of the Barkhausen noise during a magnetization reversal is the magnetic induction B, and B versus H is the hysteresis loop. Figure 1 documents the

influence of different microstructures (ferrite/ martensite) and Figure 2 presents the influence of load-induced or residual mechanical stresses. If we assume that the applied magnetic field is tangentially oriented to the magnetized materials surface the field H_t is changed continuously using a sinusoidal time function ($H_t = H_{Max} \times \sin(2 \pi f t)$; t - time, f - magnetizing frequency 10^{-3} Hz $\leq$ f $\leq$ 500 Hz, $H_{Max} \leq$ 100 A/cm, depending on the material). So called 'magnetic hard' materials, like a martensitic steel microstructure, have larger coercivity (H_t-value at B=0) and smaller remanence (B-value at H_t=0). In case of compressive stresses the hysteresis is sheared and tensile stress generates a slighter curve. Whereas the hysteresis - by definition - is measured by a coil surrounding the specimen under inspection, more suitable pick-up techniques for local, spatially resolved ND-testing have yet to be developed.

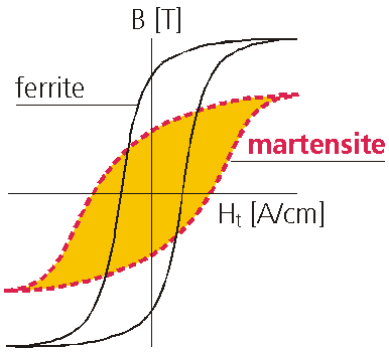

Figure 1 Hysteresis loop and influence of microstructure

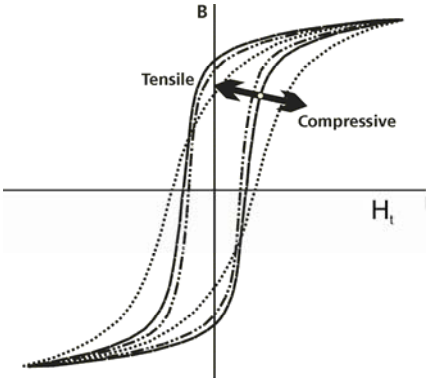

Figure 2 Hysteresis loop and influence of mechanical stress

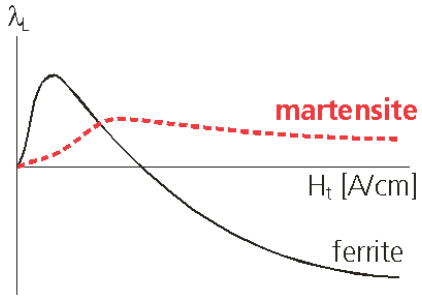

Fiogure 3 Lengthwise magnetostriction and influence of microstructure

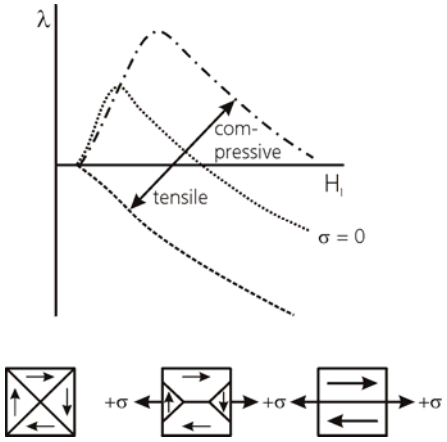

Figure 4 Lengthwise magnetostriction and influence of mechanical stress

Ferromagnetic materials also show the property of magnetostriction. [5] When exposed to a magnetic field, its dimension changes. The effect can be measured as a function of the applied magnetic field in profile-curves ($\lambda(H_t)$ or $\lambda_L(H_t)$, L-lengthwise magnetized cylindrical specimen) by using strain gages (Figure 3 and Figure 4). The

inverse effect is the spontaneous magnetization of a virgin ferromagnetic material exposed to a mechanical stress field. This is the reason of the stress sensitivity of micromagnetic NDT [9-11]. In the lower part of Figure 4, according to a 4-domain model [5], the effect of increasing tensile stress on the domain wall movement is discussed. The domains with magnetization direction in the tensile stress direction are preferred.

2. Measuring Techniques, Transducers and Sensors in Detail

For the development of non-destructive (ND)-techniques, some special principles have been identified from the above mentioned basic physical facts, providing a selective interaction with the microstructure and stress fields. These are particularly micromagnetic techniques.

Depending on the magnetic process performance irreversible and reversible processes have to be distinguished [12]. Techniques using irreversible processes take advantage of the non-linearities of the hysteresis which are the result of the above mentioned Bloch-wall jumps and rotational processes [13]. A distortion factor K can be derived from a Fourier analysis of one period of the time-signal of the magnetic tangential field strength H_t which is measured by a Hall element. K is the geometrical average (root-mean-square-value) of the power of the upper harmonics, normalized to the power of the fundamental [14].

Because of the nonlinear hysteresis behavior, the time domain signal of the tangential magnetic field strength is a superposition of the above mentioned fundamental and higher harmonics. The signal is analyzed by a Fast Fourier Transform. Only the fundamental and the odd order complex valued coefficients need to be calculated because of the hysteresis symmetry. The distortion factor K is defined as shown in Figure 5.

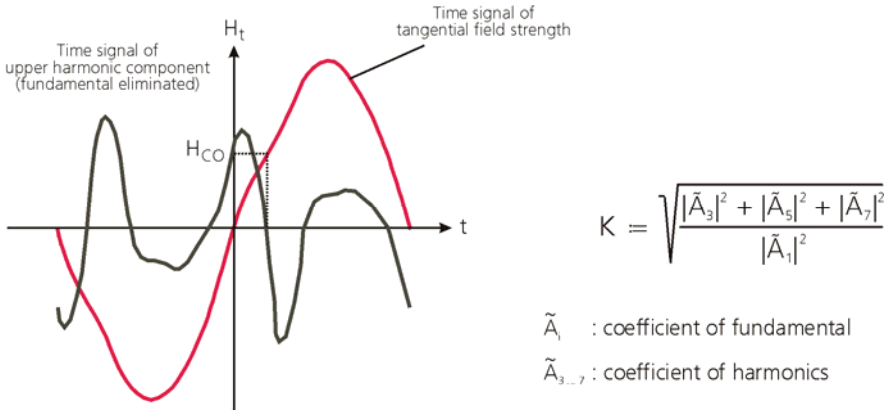

Figure 5 Fourier analysis of the magnetic tangential field

By empirical investigations it was shown that from the time dependence of the sum of all harmonics above the fundamental a coercivity value H_{CO} may be derived. This value correlates with the hysteresis coercivity H_C. The investigations are confirmed by other authors [15]. Thus, using this measurement of the tangential field strength, with

only one sensor, two independent parameters may be derived. The spatial resolution is a few mm. The depth that is analyzed is controlled by the penetration depth of the applied field H_t which in turn depends on the magnetizing frequency f.

The Barkhausen noise is magnetically received directly by a pick-up air-coil, a ferrite-core-coil, or a tape recorder head as induced electric voltage pulses. After low-noise pre-amplification (60 dB fixed), band-pass filtering (cut-off frequencies to be adjusted), rectifying, low-pass-filtering in order to receive the envelope of the high-frequency content of the noise, and final amplification (variable up to 60 dB), the so called magnetic Barkhausen noise profile-curve $M(H_t)$ is obtained [16]. This type of technique was proposed by Matzkanin [1].

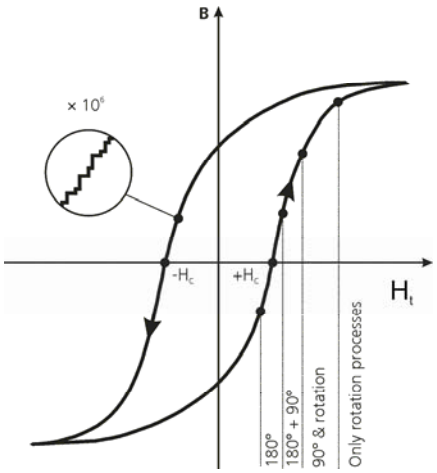

Figure 6 Hysteresis, Barkhausen noise, micromagnetic events: Bloch wall jumps, rotation processes.

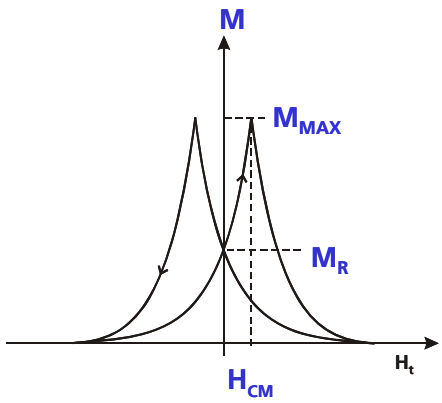

Figure 7 Magnetic Barkhausen noise profile curve

The spatial resolution is restricted by the sensor geometry and is measured laterally as a so called ‘effectiveness distance’, according to a DIN-standard [17]. The mm-range can be achieved by using standard pick-up air coils. The band pass filter is needed to suppress the large magnitude of the fundamental magnetizing frequency in the received signal in addition to its higher harmonics. This effect is stronger for magnetic soft materials than for hard ones. For soft materials an essential higher harmonic component up to the 7th order is observed. The lower cut-off frequency of the band pass filter therefore has to be adjustable, depending on the material under inspection. It should be mentioned here, that this measure to suppress disturbing noise and to receive the random Barkhausen noise limits the analyzing depth for technical steels in general to a depth of ≈ 2 mm. Because the analyzing depth of the above mentioned distortion factor the measurement is limited only by the magnetizing frequency, this parameter completes the information of the Barkhausen noise to a larger analyzing depth. Because of the random character of the Barkhausen-noise a large natural scatter in the data is observed due to small magnetic fluctuations from the environment superimposed on the driving field. Time averaging (up to ten magnetizing cycles) is a help to obtain reliable data. In process applications at higher inspection speeds, the effect can hinder the use of Barkhausen-noise.

Figure 6 shows a hysteresis loop as a continuous curve. Only with a higher amplification the fact of the discontinuous magnetization in Bloch wall jumps is revealed. The Figure also documents the fact of the interaction of the different Bloch-wall types at different magnetic field amplitudes. In the vicinity of the coercivity mainly the 180° walls contribute with their jumps to the magnetizing process. The 90° walls need more energy for movement and therefore their contribution to magnetization is in the knee region of the hysteresis followed by rotation processes. In Fig. 7 a Barkhausen noise profile-curve ($M(H_t)$) is shown and the measuring parameters are presented. For some steel grades we can observe profile-curves with up to three peaks per magnetizing half-cycle, depending on the materials microstructure. Besides the different peak maxima (M_{Maxi}, i=1,..,3) their separation (H_{CMi}) as well as different half-width-values (for instance $\Delta_{M50\%}$) are measured. For residual stress characterization (see Figure 8), the peak values are measured as a function of compressive and tensile stress, M_{Max} versus stress σ. The magnetic stress sensitivity of a material microstructural state is characterized by the function $\Delta M_{Max}(\sigma)/\Delta\sigma$ i.e., the inclination of the curve $M_{Max}(\sigma)$ at $\sigma = 0$. The fact of the decreasing of the peak amplitude of the Barkhausen noise at higher tensile stress levels is observed at a mechanical stress value in the tensile regime at which the magnetostriction curve under magnetization (see Figure 4) starts directly with negative values.

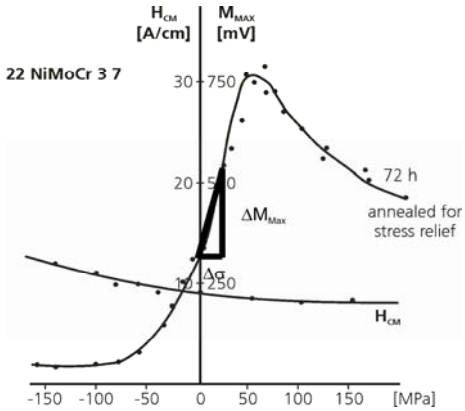

Figure 8 Barkhausen noise peak maximum and peak separation as function of mechanical stress and stress sensitivity $\Delta M_{Max} / \Delta\sigma$ of the German pressure vessel steel 22 NiMoCr 37 after welding and 72h stress relief annealing

Due to magnetostrictive effects, Barkhausen-events excite, in their vicinity, pulsed magnetostrictive strains which result in magnetostrictively excited acoustic emission signals named acoustic Barkhausen noise. [18] This is also known as MAE - magnetomechanical-acoustic-emission [19, 20]. The acoustic emission (AE) is received by narrow band, sensitive AE-transducers. Nevertheless, a high amplification of ~ 80 - 100 dB is needed and the technique is sensitive to disturbing noise. Typical AE-signal analysis equipments like RMS-voltmeters, $<A(H_t)>$, or energy-modules, $<A^2(H_t)>$, are in use. The received information is discussed using the so called profile-curves as a function of the applied magnetic field H_t. The spatial resolution is controlled by the extent of the applied magnetizing field in the material and depends strongly on the magnetizing facility. Beside the typical maxima and minima in the profile-curves,

which are characteristic parameters, their corresponding H_t- values, i.e. peak separations, zeros and peak half-width-values are evaluated. Because of its sensitivity for disturbing noise, the technique can reliably be applied only in the laboratory. Nevertheless investigations with this technique are of interest for comprehensive interpretation studies because here only the information of 90° Bloch wall movement and their interaction with the microstructure is observed.

Applying reversible magnetic techniques, the material is magnetized with a much smaller field strength amplitude ΔH compared to the coercivity (H_C) of the material. The magnetization follows linearly the magnetic field. Therefore, all eddy current techniques using low electric currents in the pick-up coil, resulting in small magnetic fields ΔH ($\Delta H << H_C$), are reversible techniques. Parameters influencing the coil impedance are the testing frequency f_Δ, the electrical conductivity σ_{el} and the incremental permeability μ_Δ. The latter depends on the magnetic history of the specimen under inspection. An eddy current impedance spectroscopy is performed by tuning the frequency from high to low values. (σ_{el}, μ_Δ) - gradients in near surface zones are sensed by changing the field penetration. The spatial resolution is the same as that for eddy current coils.

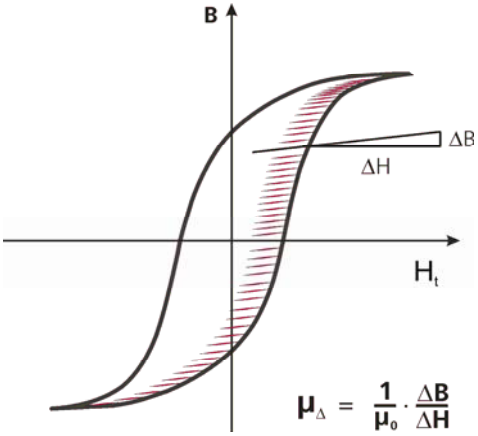

Figure 9 Incremental premeability

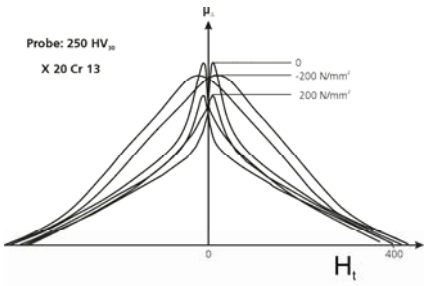

Figure 10 Incremental permeability profile curves documenting the influence of mechanical stress, steel quality X20Cr13

The incremental permeability profile-curve, $\mu_\Delta(H_t)$, as a function of a controlled applied magnetic field H_t is a well defined property of the material and independent of the magnetic prehistory as long as $H_{Max} >> H_C$ and $\Delta H << H_C$. The frequency f_Δ of the incremental field ΔH is a parameter for selecting the depth of the analyzed near surface zone; f_Δ should be chosen such that $f_\Delta \geq 100 \times f$, where f is the frequency of the applied field H_t controlling the hysteresis. $\mu_\Delta(H_t)$ is measured as eddy current impedance parallel to the hysteresis reversals. The hysteresis is modulated by the alternating field ΔH, excited by the eddy current coil. The spatial resolution is the same as that for eddy current coils. Figure 9, shows the hysteresis with the inner loops, performed by the above mentioned modulation. By definition $\mu_\Delta(H_t)$ is proportional to the inclination of each individual inner loop touching the hysteresis for magnetic field

values H_t. In Figure 10 $\mu_\Delta(H_a)$ profile-curves are presented, indicating the characteristic measuring parameters as function of mechanical stresses.

The dynamic or incremental magnetostriction profile-curve $E_\lambda(H_t)$ is the intensity of ultrasound which is excited, and received by an EMAT (Electro-Magnetic-Acoustic-Transducer), in through transmission, caused by magnetostrictive excitation as a function of the applied field H_t, controlling the hysteresis. The incremental, alternating field ΔH in this case is excited by the EMA - transmitter using a pulsed current. The magnetostriction is modulated. (Figure 11, upper part) The spatial resolution - depending on the transmitter design - is of the order of ~ 5 mm. In order to achieve such a spatial resolution, an EMA - receiver was designed to transform the ultrasonic signal into an electical signal using the Lorentz-mechanisms [21]. Figure 11, lower part, presents a half-cycle of the dynamic magnetostriction profile-curve $E_\lambda(H_t)$ in the magnetic field range $<$ 300 A/cm. The amplitude value of the first peak as well as the corresponding tangential magnetic field value as well as the H_t-field position of the minimum are sensitive quantities for materials characterization.

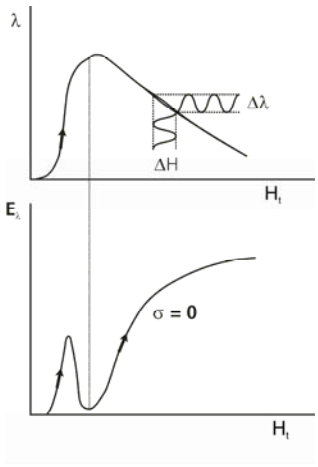

Figure 11 Dynamic or incremental magnetostriction

The micromagnetic measurements are performed by an intelligent transducer consisting of a handheld magnetic yoke together with a Hall-probe for measuring the tangential magnetic field strength and a pick-up coil for detecting the magnetic Barkhausen noise or the incremental permeability. Normally a U-shaped magnetic yoke is used, which is set onto the surface of the material under inspection, i.e. the ferromagnetic material is the magnetic ‘shunt’ of the magnetic circuit. Therefore all the well known design rules for magnetic circuits have been observed. The magnetic resistance of an air gap in a magnetic circuit is the largest possible magnetic resistance. Therefore design measures have to limit a fluctuating lift off, especially, if the transducer is manipulated along a surface. The pole shoes are made with a special shape, i.e chamfered, in order to produce a relative well defined demagnetizing field. Yoke materials with low coercivity and high saturation magnetization are used. The exciting coils are designed with an optimal fill-factor, in order to avoid additional leakage fluxes. The position of the coils is as near as possible to the pole shoe’s ends. The exciting coils are driven by a biploar power supply with adjustable output current

respectively voltage amplifiers. In practice power amplifiers are available, which are controlled by a sine generator adjustable in the exciting frequency f. In order to control the maximum received magnetic field strength H_{Max} in the material and to produce well defined dynamic magnetic reversals, a Hall element is applied tangential to the surface and symmetric to the pole shoes. In a closed loop, the field value is compared with a given value and adjusted with a feedback circuit.

The mathematical methodology of the Micromagnetic-, Multiparameter-, Microstructure-, and stress- Analysis (3MA) in detail is described in [4]. However, a short explanation is given here according to Figure 12.

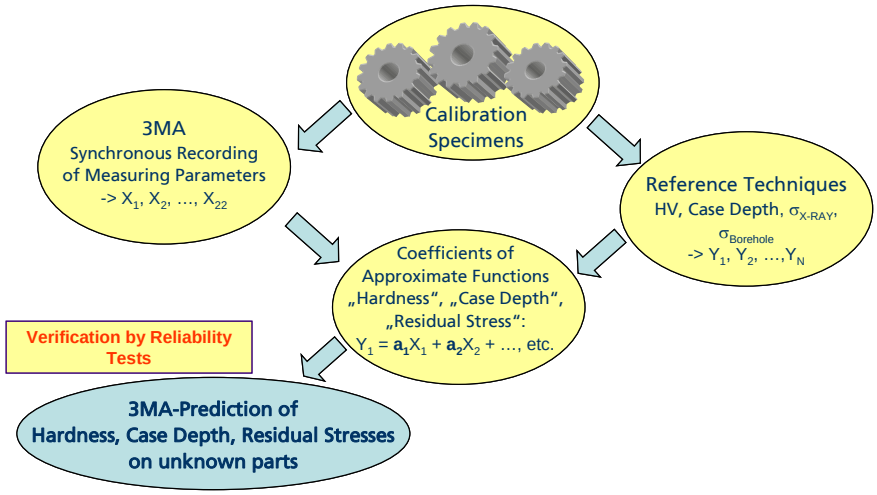

Figure 12 The 3MA-calibration

With 3MA different micromagnetic quantities, let's say X_i, i = 1, 2, 3, … are measured at 'well defined' calibration specimens. These are derived by analysis of the magnetic Barkhausen noise $M(H_t)$, the incremental permeability $\mu(H_t)$ as function of a tangential magnetic field H_t which is also analyzed and by eddy current impedance measurements at different operating frequencies. 'Well defined' here has the meaning that the calibration specimens are reliably described in reference values like mechanical hardness (according to Vickers or Brinell, etc.) or strength values like yield and/or tensile strength, or residual stress values measured, for instance, by X-ray diffraction. A model of the target function is assumed (for instance Vickers Hardness $HV(X_i)$, or strength value like $Rp0.2(X_i)$, or residual stress $\sigma res(X_i)$). This model is based on the development of the target function by using a (mathematically) complete basis function system, which is a set of polynomials in the micromagnetic measurement parameters X_i. The unknown in the model are the development coefficients, in Figure 10 called a_i. These a_i are determined in a least square algorithm, minimizing a norm of the residual function formed by the difference of the model function to the target reference values. In order to stochastically find a best approximation, only one part of the set of specimens are used for calibration of the model, the other independently selected part is applied to check the quality of the model (verification test). By using the least square approach the unknown parameters are the solution of a system of linear equations.

3MA is especially sensitive to mechanical property determination as the relevant microstructure is governing the material behavior under mechanical loads (strength and toughness) in a similar way as the magnetic behavior under magnetic loads, i.e. during the magnetization in a hysteresis loop. Because of the complexity of microstructures and the superimposed stress sensitivity there is an absolute need to develop the multiple parameter approach.

Whereas the first generation of 3MA equipments was basing on the magnetic Barkhausen noise and magnetic tangential field analysis only, 3MA equipment exist now in the forth generation (see Figure 13) also integrating incremental permeability and eddy current impedance measurements. More than 100

installations are in use in different industrial areas. This mainly covers the steel and machinery building industries. First steps into a standardization direction are gone by describing guidelines by the German Electrical Engineering Society VDE [22].

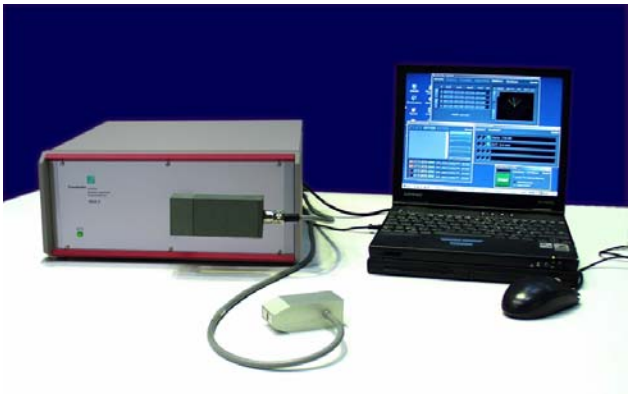

Figure 13 TCP-IP-based 3MA equipment and software in combination with a laptop

3. Applications in the steel industry

3.1 Steel Strip Inspection

A lot of experiences with 3MA in the last 2 decades were to the continuous mechanical property determination at steel strips, designed to produce car bodies [23, 24], running with a speed of 300 m/minute for instance in a continuous galvanizing and annealing line. Yield strength (Rp0.2), tensile strength (Rm), planar and vertical anisotropy parameters (r_m, Δr) are in the focus of quality assurance measures [23], all of them are defined by destructive test and cannot be measured continuously. Therefore 3MA correlations were calibrated.

Figure 14 shows a yield strength profile along a coil of 2.5 km length [24]. At the beginning and the end an unacceptable increasing of strength is detected higher than the upper acceptance level (blue line). The strength values are calculated by the 3MA approach from measured micromagnetic data. The red dots indicate the selection of specimens taken to destructive verification tests after performing NDT. The residual standard errors found by validation are in the range 4-7 % concerning the yield strength. Figure 15 shows a 3MA installation in the line of a strip producer; a robot is used to handle the transducer.

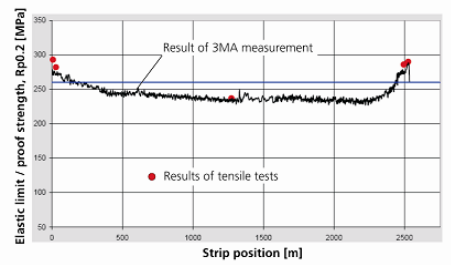

Figure 14 3MA predicted Yield strength [5]

Figure 15 3MA probe with robot at a strip line

3.2 Heavy plate Inspection

Ongoing research is to heavy plate inspection. The steel producer asks for the measurement of geometrical and mechanical properties, which have to be uniform along the product length and width, especially in the case of high-value grades used in off-shore application. Destructive tensile and toughness tests are performed by highly qualified and certified personnel according to codes and delivery conditions. The tests cannot be integrated into online closed loop control with direct feedback. To reliably test the mechanical hardness the surface must be carefully prepared by removing scale and decarburized surface layers and residual stresses are to relieve. The extraction of the test pieces and testing is very time and cost extensive. Costs in the range of several thousands Euro per year arise in a middle-sized heavy plate plant only by destruction of the test pieces.

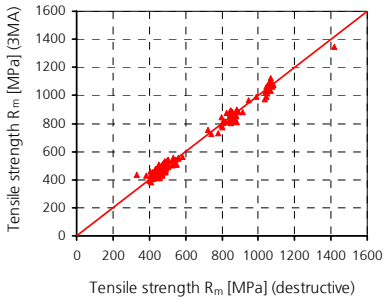

Figure 16 Tensile strength predicted by 3MA [24]

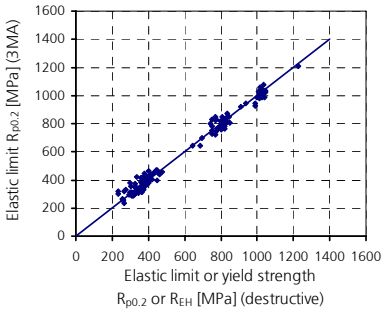

Figure 17 Yield strength predicted by 3MA [24]

In case of a mother plate of several meters length the edges are usually subjected to other cooling conditions than the rest. Indeed, especially the plate ends are known to cool faster, generating an undesired increase in tensile strength Rm and yield strength Rp0.2. State-of-the-art is to cut-off the plate edges with non-conform properties based on empirical values concerning the cut-off length. As the destructive tensile test follows directly after the cut-off process of the edges, only the result of these tests can reveal the selection of a not appropriate cut-off length. This results in high costs due to reworking, pseudo-scrap and delayed shipment release; the European steel producers

estimate their annual costs in the range of 11 million Euros. Knowing exactly the contour of the zone with unacceptable material properties would allow an open loop control of the cut-off process. Therefore heavy plate producers will replace the destructive quality inspection of test pieces by a NDT technology [24] applying 3MA (see Figure 16 and 17). By a manufacturer-specific calibration residual standard errors of 10 MPa (Rm), 20 MPa (Rp0.2), and 4HB in the Brinell hardness can be obtained. It should mention here that in the 3MA calibration also other measuring quantities can be integrated so far they provide other independent information, for instance elastic properties. By using ultrasonic waves propagating in thickness direction, i.e. a compressive wave excited by a piezoelectric transducer (index L) and two linearly polarized shear waves (polarized in, index SHR, and transverse, index SHT, to the rolling direction) excited by a EMAT, normalized time-of-flight quantities can be derived describing crystallographic texture effects. Taking into account these quantities (t_{SHR}/t_L, t_{SHT}/t_L, $(t_{SHR}-t_{SHT})/t_L$) together with the micromagnetic parameters then a regression result is obtained again reducing the residual standard error.

4. Application in Automotive and Machinery Building Industry

4.1 Car Engine casting

To reduce the weight of the power supply unit the car combustion engines cylinder crankcases can be made of cast iron with vermicular graphite (GJV), because this material in a Diesel engine allows a higher loading pressure even by reduced wall thickness. However, the service live of machining tools is during processing an engine block made from GJV substantially smaller compared with a block from cast iron with lamellar (flake) graphite (GJL).

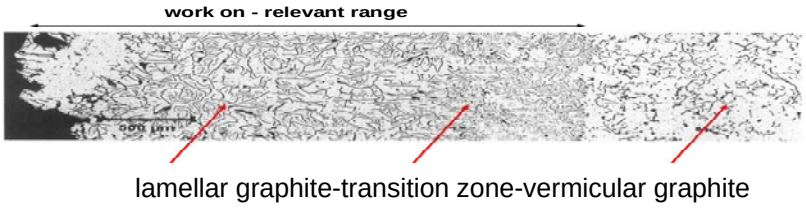

Figure 18 Microstructure gradient obtained in a cylinder region of a cast engine [25]

This disadvantage can be eliminated by an innovative casting technology that produces a continuous microstructure gradient in the cast iron from lamellar graphite at the inner surface of the cylinders to vermicular graphite in radial direction. By implementing some chemical additives into the core of the mould which can diffuse in the cast iron during the solidification process in the mould the gradient with a continuous transition from lamellar graphite and finally vermicular graphite is obtained. However, the technology can only be used by the casters so far the gradient quality can be characterized and monitored by NDT. Figure 18 documents in a micrograph such a

gradient beginning at the left side with cast iron (inner cylinder surface) and lamellar graphite followed by a transition region and vermicular graphite on the right side.

3MA techniques always cover a certain analysing depth depending on the magnetizing frequency and geometrical parameters of the magnetization yoke, etc. So far the gradient has different graphite compositions within the analysing depth, 3MA quantities should be influenced. Based on measurements at an especially designed calibration test specimen set 3MA quantities were selected to image the gradient with optimal contrast. As reference quantity to calibrate 3MA the local thickness of the GJV-layer was evaluated by using micrographs and optimized pattern recognition algorithms in the microscope. A special designed transducer head was developed to scan the cylinder surface by line scans in hoop direction and rotating the head, then shifting the head in axial direction to perform the next line scan. Figure 19 and Figure 20 show as example the coercivity images derived from the tangential field strength evaluation (H_{CO} in A/cm) and line scans covering an angle range of 190°.

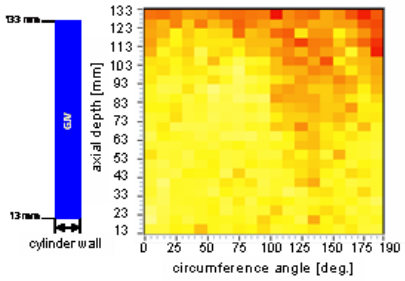

Figure 19 Coercivity image of a reference block made from GJV

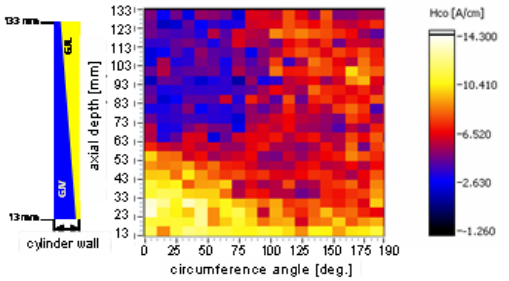

Figure 20 Coercivity image of a block with GJV/GJL gradient

Combining different 3MA quantities in a multiple regression the thickness of the GJL layer was predicted. A regression coefficient of R^2= 0.93 and a residual standard error of σ = 0.06 mm was obtained [25].

4.2 Wheel Bearing Inspection

The fixation of the inner ring of wheel bearings is performed by a wobble riveting process. As a consequence a residual stress is built up in the ring which may not exceed a limit value of about 300 MPa to get a perfect quality.

The usual technique to inspect the residual stress state is X-ray diffraction which is destructive in nature because it requires a preparation of the test location. Furthermore it can only be performed statistically. The 3MA technique allows a fast non-destructive estimation of the residual stress level (Figures 21, 22). After a calibration step by using X-ray reference values a 100% quality inspection of these parts is possible. The calibration procedure requires a coincidence of the 3MA and X-ray calibration positions because residual stress varies along the circumference. That means the 3MA data have to be recorded in a first step before the X-ray test location is prepared by etching. According to Figure 22 the residual standard error in the calibration is in the 20 MPa range. Besides the residual stress additionally the surface hardness can be measured.

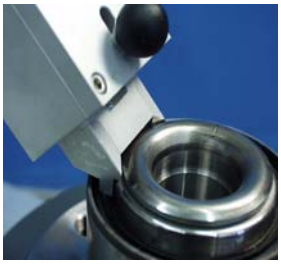

Figure 21 3MA-Probe at test location

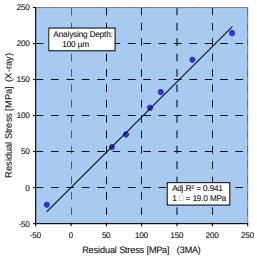

Figure 22 Residual stress calibration

4.3 Evaluation of Microstructure and Stress Gradients

Machined parts in most of the cases have more or less steep gradients in their properties near the surfaces. To improve the lifetime of mechanical highly stressed machinery components the bearing areas are surface-hardened from the µm- up to the millimetre range depending on the requirements and on the hardening technology.

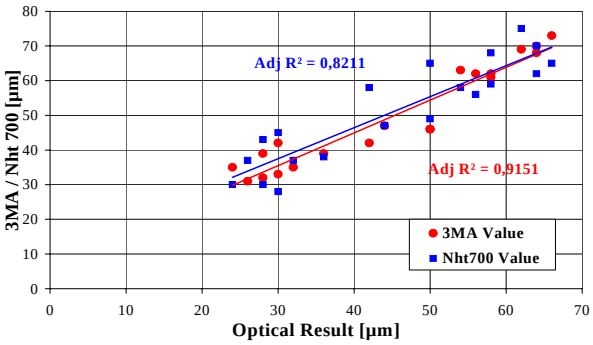

Fig.23 Comparison of nitrating hardening depth measured by 3MA and nitrading hardening depth Nht 700 (Vickers) versus optical result

Additional surface finishing by grinding can superimpose surface near defects of microstructure and residual stresses which can result in a part breakdown. To inspect the production quality in many cases not only the properties immediately at the surface but also information of the properties below the surface are desired. 3MA is an effective tool to investigate the properties near the surface as well as the range below the surface up to several millimetres in depth.

One example of a 3MA application in industry is the determination of nitrating hardening depth Nht of piston rings on the flank side and on the tread surface. Typical values of nitrating hardening depth are between 60 and about 100 µm. It is found by the customer that the reproducibility of the non-destructive values of hardness and hardening depth in piston rings is better than the conventional testing by a metallographic Vickers hardness test (Nht700), as can be seen in Figure 23 [26]. The reason of that behaviour seems to be the difference in the lateral resolution of the

conventional and the non-destructive testing method. Due to a diameter of the 3MA receiver coil of about 2 mm the 3MA values are covering a much larger inspection area. Fast data evaluation by 3MA allows a complete production feedback control.

The occurrence of grinding defects, e. g. in gear wheels, is a main problem since many years which is caused by too much heat input during the grinding process. Modern grinding tools allow much higher grinding speed compared to former machines but on the other side this can result in more defects. To get information on the quality of grinded microstructure states the common method in industry is the nital etching technique. Grinding defects are indicated by the discoloration of the surface. This technique is effective as long as the surface information is sufficient to estimate the quality. But it fails if in a preceding production step defects are produced below the surface which are covered in the next production step by a perfect finishing. Several examples of defective gear wheels investigated by hole drilling method and X-ray diffraction have shown that in a depth of 100 µm high tensile stresses up to several 100 MPa can be present whereas at the surface a perfect compressive state of several hundred MPa has been found. These hidden defects cannot be detected by nital etching. As a consequence after some time small cracks are covering the surface due to stress-relieve even without a mechanical load.

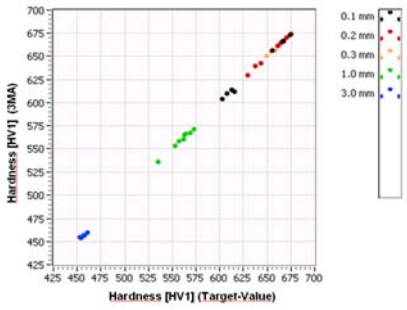

Figure 24 Hardness calibration at various depths; hardness values determined by 3MA versus target values

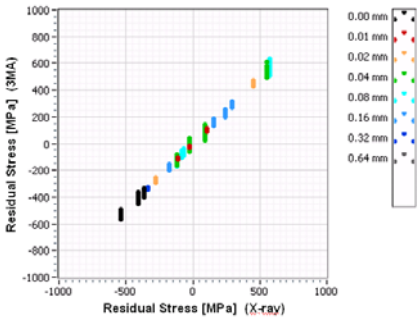

Figure 25 Residual Stress calibration at various depths; RS values determined by 3MA versus X-ray reference values

Since several years IZFP has gained experience in the non-destructive detection and quantitative evaluation of such grinding defect gradients by 3MA in cooperation with industrial partners and in different research and development projects [27, 28]. After a calibration step 3MA can be used to evaluate different target values simultaneously, especially the hardness and the residual stress at the surface and in several depths below the surface (Figures 24 and 25). To get unambiguous results calibration must be done carefully. Calibration is mainly determined by well defined calibration specimens and only valid to the target ranges available by calibration. In most cases calibration is restricted e. g. to the material, to the actual machining parameters and even to the 3MA probe in use. If any variation occurs, its influence on the validation of the existing calibration has to be checked and if necessary a recalibration or extension of the existing calibration has to be performed to include any disturbances. These limitations and the calibration effort may be seen as a disadvantage of 3MA. But if an optimal calibration is developed the fast non-destructive

determination of various quality parameters which is desired concerning expensive security related parts justifies this effort.

5. Conclusion

3MA is a matured technology and a wide field of applications is given. However, besides the success story we also can find critical remarks from industrial users. These are mainly to the calibration efforts and problems of recalibration if a sensor has to be changed because of damage by wear. Therefore actual emphasis of R&D is to generalize calibration procedures.

6. Acknowledgements

The author very much appreciate to acknowledge the contribution to the result by companies as ThyssenKrupp Stahl AG, Duisburg, ArcelorMittal Research, Metz, Dillinger Hütte GTS AG, Dillingen, Halberg Guss GmbH, Saarbrücken, and Schaeffler KG, Schweinfurt.
Over years colleagues as W.A. Theine., B. Reimringer, H. Kopp, P. Schorr, E. Waschkies, R. Kern, H. Pitsch, M. Borsutzki, R. Koch, R. Becker, Ch. Rodner, A. Yashan, U. Maisl, M. Kopp, I. Altpeter, K. Szielasko, M. Rabung, R. Tschuncky, F. Niese, G. Hübschen, H.-J. Salzburger, and B. Wolter have contributed continuously by their innovative ideas and developments to complete the 3MA approach. All of them, I have to thank very much.

References

[1] G.A. Matzkanin, et al., The Barkhausen Effekt and its Application to Nondestructive Evaluation, *NTIAC report* 79-2 (1979) (Nondestructive Testing Information Analysis Center, San Antonio, Texas) 1-49.
[2] W.A. Theiner, E. Waschkies, Method for the non-destructive determination of material states by use of the Barkhausen-effect (in German), Patent DE 2837733C2 (1984).
[3] G. Dobmann et al., Barkhausen Noise Measurements and related Measurements in Ferromagnetic Materials; in Volume 1: Topics on Non-destructive Evaluation series (B.B. Djordjevic, H. Dos Reis, editors), Sensing for Materials Characterization, Processing, and Manufacturing (G. Birnbaum, B. Auld , Volume 1 technical editors), *The American Society for Non-destructive Testing* (1998) ISBN 1-57117-067-7
[4] I. Altpeter, et al., Electromagnetic and Micro-Magnetic Non-Destructive Characterization (NDC) for Material Mechanical Property Determination and Prediction in Steel Industry and in Lifetime Extension Strategies of NPP Steel Components, *Inverse Problems* 18 (2002) 1907-1921.
[5] B.D. Cullity, Introduction to magnetic materials, (Addison- Wesley, London, 1972).
[6] E. Kneller, Ferromagnetismus, (Springer, Berlin, 1966).
[7] A. Seeger, Moderne Probleme der Metallphysik, (Springer, Berlin, 1966), Vol. 2.
[8] J.C. McClure, Jr., K. Schröder, The Barkhausen Effect, in Critical Reviews in Solid State Sciences, **6**, 45, (1976).
[9] M.J. Sablik, G.L. Burkhart, H. Kwun, D.C. Jiles, A model for the effect of stress on the low-frequency harmonic content of the magnetic induction in ferromagnetic materials, J. Appl. Phys. 63, 3930 (1988).
[10] G.L. Burkhart, H. Kwun, Measurement of residual stresses aroun a circular patch weld using Barkhausen noise, in Review of Progress in Quantitative NDE, Vol. 8B, D. O. Thompson, D. Chimenti, Eds. (Plenum Press, New York, 1989), p. 2043.

[11] D.C. Jiles, Review of magnetic methods for nondestructive evaluation, NDT International, Vol. 21, 311 (1988).
[12] G. Dobmann et al., Progress in the Micromagnetic Multiparameter Microstructure and Stress Analysis (3MA), in Nondestructive Characterization of Materials III, P.Höller, V. Hauk, G. Dobmann, C. Ruud, R. Green, Eds.(Springer, Berlin, 1989), p. 516.
[13] D.C. Jiles, Microsttructure and stress dependence of the magnetic properties of steels, in Review of Progress in Quantitative NDE, Vol. 9, D. O. Thompson, D. Chimenti, Eds. (Plenum Press, New York, 1990), p. 1821.
[14] G. Dobmann, H. Pitsch, Magnetic tangential field strength inspection a further ndt-tool for 3MA, Ibid 12, p. 636.
[15] G. Fillon; M.Lord; J.F. Bussière, Coercivity Measurement from Analysis of the Tangential Magnetic Field, in Nondestructive Characterization of Materials IV, C. Ruud, J.F. Bussière, R. Green, Eds., (Plenum Press, New York, 1990) pp. 223 - 230.
[16] W.A. Theiner et al., The 3MA-testing equipment, application possibilities and experiences, Ibid. 12, p. 699.
[17] DIN 54 140 part 2; Inductive Techniques, Nomenclature.
[18] W.A. Theiner, E. Waschkies, Verfahren zur zerstörungsfreien Feststellung von Werkstoffzuständen unter Ausnutzung des Barkhausen-Effektes, Patent DE 2837733C2, 1984.
[19] D.J. Buttle, M.T. Hutchings, Residual stress Measurements at NNDTC, British Journal of NDT, Vol. 34, No 4, 175 (1992)
[20] A.J. Allen, D.J. Buttle, From Microstructural Assessment to Monitoring Component Performance - A Review Relating Different Non-Destructive Studies, in Nondestructive Characterization of Materials V, T. Kishi, T. Saito, C. Ruud, R. Green, Eds. (Plenum Press, New York, 1992), pp. 9 - 30.
[21] R. Koch, P. Höller, A modulus for the evaluation of the dynamic magnetostriction as a measured quantity for 3MA, Ibid 12, p. 644.
[22] VDI/VDE guidelines 2616, Hardness testing of metallic materials under non-standardized methods, testing of ferromagnetic materials with the KEMAG method, **K**ombination **e**lektro**mag**netischer Prüfverfahren = Combination of electromagnetic testing methods
[23] M. Borsutzki, Process-integrated determination of the yield strength and the deep drawability properties rm and Δr on cold-rolled and hot-dip-galvanized steel sheets (in German); Ph.D. thesis, Saar University, Saarbrücken, Germany, 1997.
[24] B.Wolter, G. Dobmann, Micromagnetic Testing for Rolled Steel, European Conference on Non-destructive Testing (9) (2006) Th. 3.7.1, 25.-29. 09. 2006, Berlin.
[25] M. Abuhamad, I. Altpeter, G. Dobmann, M. Kopp, Non-destructive characterization of cast iron gradient combustion engine cylinder crankcase by electromagnetic techniques (in German), Proceedings of the DGZfP-Annual Assembly (2007), Fürth.
[26] IZFP Annual Report, (2004), Saarbrücken, Germany.
[27] W. A. Theiner et al., Process Integrated Nondestructive Testing For Evaluation Of Hardness; in the proceedings of the 14th World Conference on Nondestructive Testing (14th WCNDT), (1996) 573, New Delhi, India.
[28] B. Wolter et al., Detection and Quantification of Grinding Damage by Using EC and 3MA Techniques, in the proceedings of the 4th International Conference on Barkhausen Noise and Micromagnetic Testing, 03-04 July 2003, Brecia, Italy, 159-170.